Research Square

Preprints are preliminary reports that have not undergone peer review.
They should not be considered conclusive, used to inform clinical practice,
or referenced by the media as validated information.

Distinct Genomic and Immune Characteristics Define Therapeutic Opportunities Across Rare Non-Squamous Cell Carcinoma Sinonasal Malignancies

Conor E. Steuer
Emory University
Brandon Wummer
Emory University
Tolulope Adeyelu
Caris Life Sciences
Andrew Elliott
Caris Life Sciences
Farah Abdulla
Caris Life Sciences
Emily Barrow
Emory University
Anthea L. Hammond
Emory University
Nicole C. Schmitt
Emory University
Harry M. Baddour
Emory University
C. Arturo Solares
Emory University
Dong M. Shin
Emory University
Yong Teng
Emory University
Jennifer Johnson
Jefferson Health
Charalampos S. Floudas
National Cancer Institute, National Institutes of Health
Daniel Lubin
Emory University

Nabil F. Saba

nfsaba@emory.edu

Emory University

Article

Keywords:

Posted Date: November 20th, 2026

DOI: https://doi.org/10.21203/rs.3.rs-11436576/v1

License: This work is licensed under a Creative Commons Attribution 4.0 International License. Read Full License

Additional Declarations: Competing interest reported. : Dr. Nabil Saba reports funding through federal grants UG1 CA233247, U54 CA274513, and grants from Exelixis and BMS, and having compensated or non-compensated advisory role with: Astra Zeneca, Eisai Medical, Exelixis, Merck, Merck EMD Serono, Pfizer, Kura, Vaccinex, CUE, BionTech, GSK, TOSK, Seagen, Flamingo, Infinity, Inovio, Aveo, Medscape, Onclive, Uptodate, BMS, J&J, Surface Oncology, Urogen, Summit, Guidepoints, Astex, Imugene, Faron Pharmaceutical, Coherus, Adagene, Fulgent, Reddy Laboratories, Merus, Springer, Nanobiotix, Taiho. Dr. Nikki Schmitt reports research funding from Taiho Oncology, and consulting funding for Johnson & Johnson, GeoVax, Aspargo Labs. Drs. Adeyelu, Elliott, and Abdulla report employment and stocks with Caris Life Sciences.

Abstract

Purpose

To comprehensively characterize the genomic, transcriptomic, immune, and clinical features of rare non-squamous cell carcinoma sinonasal malignancies (NSCCSM) and identify histology-specific biomarkers and therapeutic vulnerabilities. Using 238 tumors, this represents the largest known integrated genomic and immune sequencing analysis of NSCCSM to date, providing a framework for biomarker-driven and precision therapeutic approaches in these rare malignancies.

Experimental Design:

We performed a retrospective analysis of 238 NSCCSM specimens from the Caris Life Sciences database using next-generation sequencing, whole-transcriptome sequencing, and immunohistochemical biomarker assessment. Tumor mutational burden, microsatellite instability (MSI), PD-L1 expression, immune cell infiltration, and immune regulatory signaling were evaluated across histologic subtypes. Real-world overall survival outcomes were obtained from insurance claims data and analyzed according to histology and immunotherapy exposure.

Results

Distinct molecular and immune profiles were identified across NSCCSM subtypes. Adenoid cystic carcinoma was enriched for MYB/MYBL1 alterations, whereas adenocarcinomas demonstrated greater genomic complexity involving *TP53, APC, KRAS*, and chromatin remodeling pathways. Sinonasal undifferentiated carcinomas showed frequent *TP53* mutations, *MYC* amplification, increased PD-L1 expression, and increased immune checkpoint signaling. Olfactory neuroblastomas exhibited a high infiltration of NK cells, CD8 + T cells, and dendritic cells despite reduced interferon-gamma signaling. Median overall survival differed significantly by histology ($p = 0.0005$), with olfactory neuroblastoma demonstrating the longest survival and sinonasal undifferentiated carcinoma the shortest. Among immunotherapy-treated patients, PD-L1 positivity was associated with improved survival (HR 0.28, 95% CI 0.08–0.97; $p = 0.047$).

Conclusions

NSCCSM exhibit substantial genomic, immunologic, and clinical heterogeneity. Histology-specific molecular characterization may facilitate biomarker-driven therapeutic development and inform future precision treatments.

Introduction

Sinonasal tumors (SNTs) are a group of rare tumors that comprise less than 3% of all head and neck malignancies. Although the clinical course and survival outcomes vary with tumor type, SNTs are often

associated with high-grade morphology and an aggressive clinical course. Management of these tumors is challenging given the heterogeneous biology within the context of rare diseases. In addition, adequate local therapy is hindered by their anatomic presentation and frequent involvement of functionally critical structures such as the orbit or skull base. SNTs often present with nonspecific symptoms and are diagnosed at advanced stages with limited treatment options. Squamous cell carcinoma (SCC) accounts for approximately 50–60% of sinonasal malignancies, whereas rare non-squamous histologies remain poorly studied at the molecular and clinical levels [1].

Non-squamous cell carcinoma sinonasal malignancies (NSCCSM) are a rare and diverse subset of SNTs and include adenoid cystic carcinoma, sinonasal adenocarcinoma (AD), sinonasal undifferentiated carcinoma (SNUC), and olfactory neuroblastoma (ONB). ACC is one of the most common sinonasal carcinomas and is characterized by frequent perineural invasion, distant metastasis, and resistance to conventional systemic therapies [2]. Molecularly, ACC is characterized by recurrent alterations involving *MYB* or *MYBL1*, most commonly through *MYB::NFIB* or *MYBL1::NFIB* rearrangements, although reported frequencies vary by detection method[3]. This fusion often corresponds to rapid tumor proliferation, angiogenesis, and worse survival [4]. In addition, activating *NOTCH1* somatic mutations were identified in 14% of primary ACC and have emerged as clinically important biomarkers often associated with high-grade transformation, metastatic progression, and worse overall survival (OS) [5, 6]. Conversely, *PD-L1* expression in ACC is generally low or absent, which may contribute to limited response to immune checkpoint inhibition [7, 8].

Similarly, SNUC is a rare and highly aggressive SNT for which no validated prognostic biomarkers or standardized targeted treatments currently exist [9]. Case series have identified recurrent mutations such as *IDH2* and *SMARCB1*, both of which are associated with a hypermethylator phenotype and worse prognosis [10, 11]. In addition, the tumor immune microenvironment (TIME) in SNUC is characterized by infiltration of naïve B cells, CD8 memory T cells, and regulatory T cells along with increased expression of exhaustion markers such as LAG3, pointing to a potential role of immune targeted approaches in this disease [12, 13]. Comparatively, ONB originates from the olfactory epithelium and has diverse genetic and epigenetic alterations. *IDH2* mutations have been identified in approximately 5–17% of ONB cases and have been associated with aggressive clinicopathologic features and worse survival [14, 15]. Recurrent *IDH2* mutations are important clinically as they are associated with aggressive tumor behavior and represent therapeutically actionable alterations. The TIME of ONB is characterized by abundant tumor-infiltrating lymphocytes and variable differentiation that may impact its clinical prognosis [16, 17]. Furthermore, increased *PD-L1* expression has been identified, suggesting potential therapeutic relevance for ICI-based approaches [18].

In SCC, recent prospective randomized data from EA3163 study supported the role of induction chemotherapy in organ preservation for patients with orbit or base of skull invasion [19]. Similar approaches in NSCCSM, such as the SINTART-1 trial, have suggested a valuable role of induction chemotherapy in the management of these tumors, especially SNUC [8]. However, clinical outcomes remain poor with NSCCSM having a 5-year OS of 47–54% and progression-free survival (PFS) of 33–36% [20]. No universally accepted systemic treatment paradigm exists for NSCCSM, largely because the rarity and biologic heterogeneity of these tumors have limited the feasibility of clinical trials. Although recurrent genomic alterations in SNTs have increasingly been identified, most prior studies have focused on individual histologic subtypes, and

comparative analyses evaluating molecular, immune, and clinical characteristics across NSCCSM remain limited.

In this study, we performed a comprehensive genomic and transcriptomic analysis of 238 NSCCSM samples from the Caris database with the purpose of better characterizing the molecular landscape and heterogeneity of these rare tumors to help identify clinically important biomarkers which may inform future targeted therapeutic approaches. To our knowledge, this represents the largest integrated genomic and immune characterization of NSCCSM reported to date.

Materials and Methods

Specimens

We retrospectively examined the molecular profiles of non-squamous cell sinonasal malignancy specimens that underwent next-generation sequencing [21] of DNA (592-gene panel or whole exome sequencing [WES]) and whole transcriptome sequencing (WTS) in a CLIA certified clinical laboratory (Caris Life Sciences, Phoenix, Arizona, U.S.A.). This study was conducted in accordance with the guidelines of the Declaration of Helsinki, Belmont Report, and US Common Rule. In compliance with policy 45 CFR 46.101(b), this study was conducted using retrospective, de-identified clinical data, and patient consent was not required.

DNA next-generation sequencing [21]

A targeted 592-gene panel or WES was performed using genomic DNA isolated from microdissected formalin-fixed, paraffin-embedded (FFPE) tumor samples. The 592-gene panel was sequenced using the NextSeq platform (Illumina, Inc., San Diego, CA). A custom-designed SureSelect XT assay was used to enrich 592 whole-gene targets (Agilent Technologies, Santa Clara, CA). Whole exome sequencing was performed using the Illumina NovaSeq 6000 sequencer (Illumina, Inc). A hybrid pull-down panel of baits designed to enrich for 700 clinically relevant genes at high coverage and high read-depth was used, along with another panel designed to enrich for an additional > 20,000 genes at lower depth. Five hundred and ninety-two-gene and WES assays were cross-validated and showed highly concordant results. Matched normal tissue was not sequenced. Genetic variants identified were interpreted by board-certified molecular geneticists and categorized as ‘pathogenic,’ ‘likely pathogenic,’ ‘variant of unknown significance,’ ‘likely benign,’ or ‘benign,’ according to the American College of Medical Genetics and Genomics (ACMG) standards. When assessing mutation frequencies of individual genes, ’pathogenic,’ and ‘likely pathogenic’ were counted as mutations while ‘benign’, ‘likely benign’ variants and ‘variants of unknown significance’ were excluded.

RNA whole transcriptome sequencing (WTS)

FFPE specimens underwent pathology review to determine percent tumor content and tumor size; a minimum of 10% of tumor content in the area for microdissection was required to enable enrichment and extraction of tumor-specific RNA. Qiagen RNA FFPE kit (Qiagen, Germantown, MD, USA) was used, and the RNA quality and quantity were determined using the Agilent TapeStation (Agilent Technologies). Biotinylated

RNA baits were hybridized to the synthesized and purified cDNA targets and the bait-target complexes were amplified in a post capture PCR reaction. The resultant libraries were quantified, normalized and the pooled libraries were denatured, diluted, and sequenced. For transcript counting, transcripts per million molecules (TPM) were generated using the Salmon expression pipeline.

Immunotherapy-related biomarkers, signatures, and immune cell infiltration

We assessed tumor mutational burden (TMB) through NGS and WES; TMB-high (TMB-H) was defined as ≥10 mutation per megabase. Multiple platforms were used to determine microsatellite instability – high (MSI-H)/ deficient DNA mismatch repair (dMMR) status, including: immunohistochemistry (IHC) for MLH1 (M1 antibody), MSH2 (G2191129 antibody), MSH6 (44 antibody), and PMS2 (EPR3947 antibody, Ventana Medical Systems, Inc., Tucson, AZ, USA), and NGS (for tumors tested with NextSeq platform, 7,000 target microsatellite loci were examined and compared to the reference genome hg19 from the University of California, Santa Cruz). The two platforms generated highly concordant results; in the rare cases of discordant results, the MSI-H or dMMR status of the tumor was determined in the order of IHC followed by NGS. Expression of PD-L1 was assessed by IHC through 22C3 antibody (positive: tumor proportion score (TPS) ≥ 1%) or SP142 antibody (positive: ≥2+, ≥ 5%). All IHC was performed on FFPE section of glass slides. Slides were stained using automated staining techniques, per the manufacturer's instructions, and were optimized and validated per CLIA/CAP and ISO requirements. They were all evaluated by a board-certified pathologist.

The tumor immune cell infiltration was estimated by quanTIseq, a computational pipeline that uses RNA transcripts that are known to be expressed in specific immune cell types to estimate the different immune cell fraction from tumor-derived bulk RNA sequencing data deconvolution [21] while interferon (IFN) gamma scores were calculated as previously described[22].

Clinical outcomes

Real-world OS information was obtained from insurance claims data. OS was calculated from time of biopsy or start of immunotherapy to last contact. Overall survival was analyzed using the Kaplan-Meier method. Survival distributions were compared using the log-rank test, and hazard ratios (HRs) with 95% confidence intervals (CIs) were estimated using Cox proportional hazards models.

Statistics

Statistical analyses included the Mann-Whitney U test, Fisher's Exact and $\chi 2$ tests as appropriate, with p-values adjusted for multiple comparisons where appropriate (significance was set at $q < 0.05$).

Results

Patient characteristics

A total of 238 patients with rare non-squamous sinonasal tumors underwent genomic profiling and were included in the study, consisting of adenocarcinoma (n = 62), adenoid cystic carcinoma (ACC; n = 72), olfactory neuroblastoma (ONB; n = 62), sinonasal undifferentiated carcinoma (SNUC; n = 16), and other rare histologies (n = 26). Baseline demographic and clinical characteristics are summarized in Table 1. Median age at diagnosis differed significantly between tumor subtypes (p = 0.0095), with patients with ONB presenting at a younger median age compared to other histologies. Significant differences in racial composition were observed between tumor subtypes (p = 0.0025), with White patients comprising most of the overall cohort, while SNUC was relatively enriched in Asian/Pacific Islanders (11.5%, n = 3), although ONB had greater racial heterogeneity. Geographic distribution by continent also differed significantly across histologies (p = 0.0013), with most patients originating from Europe. No statistically significant differences were observed with respect to metastatic status at presentation or ethnicity.

Table 1

Baseline demographic and clinical characteristics of patients with rare non-squamous sinonasal malignancies. Comparison of demographic and clinical variables across adenoid cystic carcinoma [8], adenocarcinoma, olfactory neuroblastoma (ONB), sinonasal undifferentiated carcinoma (SNUC), and other rare sinonasal histologies. Variables include age at diagnosis, sex, metastatic status at presentation, race, ethnicity, and geographic distribution by continent. Abbreviations used: AFR, Africa; AMR, Americas; EAS, East Asia; EUR, Europe.

Age		**Adenocarcinoma**	**ACC**	**ONBs**	**SNUC**	**Others**	**p-value**
	Median age (range)	**63.5 (29–88)**	**63.0 (18–89)**	**57.0 (36–89)**	**57.5 (35–80)**	**62.0 (34–85)**	**0.0095**
Gender	Female	32.3% (20/62)	63.9% (46/72)	53.2% (33/62)	62.5% (10/16)	42.3% (11/26)	0.0043
	Male	67.7% (42/62)	36.1% (26/72)	46.8% (29/62)	37.5% (6/16)	57.7% (15/26)	
Metastatic Sites	Metastatic	38.7% (24/62)	43.1% (31/72)	58.1% (36/62)	25.0% (4/16)	46.2% (12/26)	0.0924
	Primary	61.3% (38/62)	56.9% (41/72)	41.9% (26/62)	75.0% (12/16)	53.8% (14/26)	
Race	Asian/Pacific Islander	0.0% (0/72)	0.0% (0/62)	8.1% (5/62)	11.5% (3/26)	0.0% (0/16)	0.0025
	Black or African American	13.9% (10/72)	17.7% (11/62)	1.6% (1/62)	7.7% (2/26)	0.0% (0/16)	
	Unknown/Other	26.4% (19/72)	27.4% (17/62)	40.3% (25/62)	34.6% (9/26)	50.0% (8/16)	
	White	59.7% (43/72)	54.8% (34/62)	50.0% (31/62)	46.2% (12/26)	50.0% (8/16)	
Ethnicity	Hispanic or Latino	9.7% (7/72)	4.8% (3/62)	21.0% (13/62)	7.7% (2/26)	12.5% (2/16)	0.1087
	Not Hispanic or Latino	72.2% (52/72)	72.6% (45/62)	69.4% (43/62)	65.4% (17/26)	62.5% (10/16)	
	Unknown/Other	18.1% (13/72)	22.6% (14/62)	9.7% (6/62)	26.9% (7/26)	25.0% (4/16)	
Continent	EUR	82.4% (42/51)	75.0% (33/44)	71.4% (25/35)	63.6% (7/11)	72.7% (8/11)	0.0013
	AFR	13.7% (7/51)	18.2% (8/44)	0.0% (0/35)	9.1% (1/11)	0.0% (0/11)	
	AMR	3.9% (2/51)	6.8% (3/44)	22.9% (8/35)	9.1% (1/11)	27.3% (3/11)	

*Others (n = 26) include carcinoma NOS (n = 13); not scanned (n = 8); lymphoepithelial carcinoma (n = 2); teratocarcinosarcoma (n = 2); sialadenopapillary ductal carcinoma (n = 1).

Age		Adenocarcinoma	ACC	ONBs	SNUC	Others	p-value
	Median age (range)	**63.5 (29–88)**	**63.0 (18–89)**	**57.0 (36–89)**	**57.5 (35–80)**	**62.0 (34–85)**	**0.0095**
	EAS	0.0% (0/51)	0.0% (0/44)	5.7% (2/35)	18.2% (2/11)	0.0% (0/11)	

*Others (n = 26) include carcinoma NOS (n = 13); not scanned (n = 8); lymphoepithelial carcinoma (n = 2); teratocarcinosarcoma (n = 2); sialadenopapillary ductal carcinoma (n = 1).

Comprehensive genomic profiling across rare NSCCSM

Comprehensive genomic profiling revealed distinct molecular patterns across NSCCSM subtypes (Fig. 1, **Supplemental table 1**). ACC was predominantly enriched for *MYB/MYBL1*-associated alterations (46.4%) and *NOTCH1* mutations (15.0%), whereas adenocarcinomas more frequently had alterations involving *TP53* (21.1%), *APC* (8.62%), *KRAS* (3.44%), and chromatin remodeling genes such as *KMT2C* (5.66%) and KMT2D (9.09%). ONBs exhibited recurrent alterations in *TP53* (5.9%, n = 3/51), epigenetic regulatory genes such as *SMARCA4* (3.8%), and co-amplification of 11q13 chromosome genes (*CCND1, FGF19* and *FGF4*) while SNUC histologies exhibited frequent *IDH2* (75.0%), *TP53* (62.5%), and *MYC*-amplification (18.2%). TMB-high status was more frequently found in AD (6.9%) compared to the other histologic subtypes (**Supplemental Table 1**).

Co-mutation analysis further demonstrated distinct patterns of genomic interaction within each histologic subtype (Fig. 2A-D). In ACC (Fig. 2A), *MYB* fusion co-occurred with *EP300* (log OR = 3.09, $p < 0.05$). *NOTCH1* mutations also co-occurred with other mutations like *CREBBP* (log OR = 3.72, $p < 0.01$)/*EP300* (log OR = 2.79, $p < 0.05$)/*KDM6A* (log OR = 2.97, $p < 0.05$). For adenocarcinoma (Fig. 2B), MMRd co-occurred with *BCOR* (log OR = 3.43, $p < 0.05$), *NF1* (log OR = 3.88, $p < 0.05$), and TMB-H (log OR = 5.40, $p < 0.01$). In ONB, two samples demonstrated 11q13 amplification, characterized by co-amplification of *CCND1*, *FGF19*, and *FGF4* (Fig. 2D).

Distinct Immune microenvironments of NSCCSM

Immune profiling revealed large differences in both the TIME (Fig. 3) and immune regulatory signaling (Fig. 4) across the tumor subtypes. Overall, the TIME of sinonasal tumors had relatively limited immune infiltration, although substantial differences were observed among histologic subtypes. ONBs exhibited significantly greater infiltration of immune effector cell populations, including median NK cells (8.06%), CD8 + T cells (0.49%), CD4 + T cells (2.45%), and myeloid dendritic cells (6.18%), compared with other sinonasal malignancies, whereas ACC tumors generally had lower immune cell infiltration consistent with an immunosuppressed phenotype (Fig. 3A). Despite the increased inflammatory infiltrate observed in ONBs, IFN-gamma signaling scores remained low compared to ACC (median: -0.67 vs -0.44, $p < 0.01$) and AD (median: -0.67 vs -0.41, $p < 0.01$) (Fig. 3B). The prevalence of high microsatellite instability (MSI-H) remained rare across all tumor types while the PD-L1 expression levels varied across different histological subtypes (Fig. 3C).

Expression of immune oncology–related genes also varied across histological subtypes. For instance, *LAG3* expression was significantly higher in SNUCs compared to ACC (median logTPM + 1: 3.47 vs 1.56). Overall,

ONBs and SNUC tumors demonstrated relatively increased expression of inhibitory checkpoint-associated markers, while AD and ACC generally exhibited lower expression profiles. *PD-L1* expression also varied between histologies, with higher expression observed in subsets of AD (28.6%) and SNUC (53.8%) histologies compared with ACC (3.2%) and ONB (6.7%). (Fig. 4).

To further characterize the immune landscape, the NSCCSM cohorts were stratified into IFN-High and IFN-Low groups using the global median transcriptomic IFN score. The proportion of IFN-High samples was lowest among ONBs (25%, $p < 0.001$). Across the NSCCSM cohort, IFN score was negatively correlated with myeloid dendritic cells ($R=-0.22$, $p < 0.01$) and NK cells ($R=-0.39$, $p < 0.001$). These associations were more pronounced in the ACC subgroup (myeloid dendritic cells: $R =-0.30$, $p < 0.05$; NK cells: $R=-0.46$, $p < 0.01$) (**Supplemental Fig. 1**).

Clinical outcomes across histologic subtypes

Survival analysis using real-world insurance claims data revealed substantial variation in clinical outcomes across subtypes (Fig. 5). Median overall survival [3] differed significantly between tumor types ($p = 0.0005$), with ONBs demonstrating the longest mOS at 76.0 months (95% CI, 36.0–89.4), followed by ACC at 58.2 months (95% CI, 31.9–86.3), adenocarcinoma at 29.3 months (95% CI, 18.7–35.3), SNUC at 14.9 months (95% CI, 9.0–NR), and other histologies at 30.5 months (95% CI, 15.7–68.0).

Among patients treated with immunotherapy (IO), median survival similarly varied across histologies, although differences did not reach statistical significance ($p = 0.26$) and interpretation was limited by the small sample size ($n = 28$). ONBs demonstrated the longest median survival following IO initiation at 23.4 months (95% CI, 2.9–39.6), compared with 4.2 months for ACC (95% CI, 3.9–11.1), 14.1 months for adenocarcinoma (95% CI, 1.0–43.6), 18.1 months for SNUC (95% CI, 1.7–NR), and 46.4 months for other histologies (95% CI, 7.2–46.4).

Among patients with NSCCSM treated with IO, PD-L1 positivity was associated with prolonged survival from IO initiation to last contact (HR = 0.28, 95% CI 0.08–0.97, $p = 0.047$) (**Supplemental Fig. 2A**). In contrast, tumors with higher CD274 transcript levels demonstrated only a nonsignificant trend toward improved outcomes (HR = 0.45, 95% CI 0.13–1.59; $p = 0.216$), and no significant difference was observed between IFN-High and IFN-Low tumors (HR = 0.76, 95% CI 0.24–2.41; $p = 0.638$) (**Supplemental Fig. 2B-C**).

Discussion

This study represents one of the largest comparative genomic and immune profiling analyses of rare non-squamous sinonasal malignancies to date. Rather than demonstrating a single molecular phenotype shared across these tumors, our findings identified distinct genomic and immune landscapes associated with individual histologic subtypes. Our findings support a histology-specific approach to molecular characterization and suggest that comprehensive profiling may provide clinically relevant information beyond histologic classification alone.

ACC demonstrated a molecular profile characterized by recurrent *MYB/MYBL1*-associated alterations and *NOTCH1* mutations, accompanied by an immune-poor TIME. The observed co-occurrence of *MYB* fusion

events with alterations in epigenetic regulators such as *EP300* and *KDM6A* further suggests that transcriptional and epigenetic dysregulation may contribute to ACC biology. The enrichment of MYB/MYBL1-associated alterations and *NOTCH1* mutations in ACC also has potential therapeutic implications. Therapeutic strategies targeting *MYB*-associated transcriptional programs and *NOTCH* signaling remain under investigation, with early clinical studies demonstrating that these pathways are biologically relevant but not yet established as routine therapeutic targets[23]. Our findings therefore support continued molecular characterization of ACC while emphasizing that detection of a recurrent alteration should not be interpreted as evidence of clinical actionability in the absence of prospective therapeutic validation.

Sinonasal adenocarcinomas demonstrated a more genomically complex phenotype, with recurrent alterations involving *TP53*, *APC*, *KRAS*, and chromatin-remodeling genes. The association of MMR deficiency with *BCOR*, *NF1*, and TMB-high further suggests that a subset of adenocarcinomas may harbor molecular features with therapeutic relevance. These findings support comprehensive genomic profiling in sinonasal adenocarcinoma, where alterations affecting MAPK, WNT, cell-cycle, and DNA repair pathways may identify opportunities for molecularly guided treatment or clinical trial enrollment. Importantly, the presence of potentially actionable alterations should be interpreted within the histologic and clinical context.

Our findings further support that the TIME of ONB is heterogeneous and cannot be characterized by immune-cell abundance alone. Instead, ONB may represent an immune-infiltrated but functionally constrained microenvironment. Prior genomic and immune profiling studies have showed a low TMB and limited *PD-L1* expression in ONB despite high variability in tumor-infiltrating lymphocytes, suggesting that immune infiltration may not translate into effective antitumor immunity[24]. More recent transcriptomic analyses have similarly identified T-cell infiltration alongside immunosuppressive myeloid populations, further supporting a model of immune infiltration with potentially impaired immune function. In our cohort, the coexistence of increased NK-cell, CD8 + T-cell, CD4 + T-cell, and dendritic-cell infiltration with low IFN-γ signaling provides further evidence of this discordance. Rather than categorizing ONB as an immunologically "hot" tumor, these findings suggest a more complex immune phenotype characterized by infiltration without corresponding evidence of robust inflammatory signaling. Together, these findings suggest that future studies of ONB should incorporate measures of immune activation in addition to cellular infiltration and *PD-L1* expression.

The molecular and immune phenotype observed in SNUC is also consistent with emerging recognition of SNUC as a heterogeneous group of molecularly defined sinonasal carcinomas[25]. Recent pathologic studies have emphasized that molecular alterations, including *IDH1/2* mutations and loss of *SMARCB1*, can identify biologically distinct subsets that were historically grouped under the SNUC designation. Our observation of frequent *IDH2* and *TP53* alterations, together with *MYC* amplification and increased expression of immune checkpoint-associated genes, further supports the concept that molecular profiling may refine the biologic classification of these aggressive tumors. The combination of potentially targetable genomic alterations and an immune-infiltrated or checkpoint-expressing microenvironment provides a rationale for prospective investigation of biomarker-selected treatment strategies, although the small number of SNUC cases in our cohort precludes therapeutic conclusions.

The substantial differences in overall survival across histologies further support the biologic distinction between these tumors. ONB demonstrated the longest overall survival, whereas SNUC had the shortest. Although survival following immunotherapy initiation varied across histologies, these analyses were limited by the small number of treated patients and did not demonstrate statistically significant differences. The association between PD-L1 positivity and improved survival following immunotherapy initiation is hypothesis-generating, but the lack of significant associations with *CD274* transcript levels or IFN status highlights the complexity of using individual immune biomarkers to predict therapeutic benefit in these rare malignancies.

Collectively, these findings have several implications for the clinical evaluation of rare sinonasal malignancies. Comprehensive molecular profiling may identify recurrent alterations that provide opportunities for targeted therapy or clinical trial enrollment, particularly in diseases for which standard systemic treatments remain limited. Also, molecular testing may provide information about the immune contexture of these tumors that is not captured by histology alone. The combination of genomic alterations, immune-cell composition, inflammatory signaling, and checkpoint expression may ultimately prove more informative than any individual biomarker when selecting patients for immunotherapy or rational combination approaches.

There are several limitations of this study. First, the retrospective nature of the study introduces potential selection bias and limits the ability to establish causal relationships between molecular alterations and clinical outcomes. Second, despite representing a relatively large cohort for these rare malignancies, certain histologic subgroups were limited in sample size, particularly for survival analyses involving patients treated with immunotherapy. Third, the use of real-world genomic and insurance claims data does not incorporate other variables, including disease burden, treatment sequencing, and other factors that may influence survival. Finally, the molecular and immune associations identified in this study require validation in prospective clinical studies before they can be used as predictive biomarkers.

Despite these limitations, our findings provide a framework for understanding rare sinonasal malignancies as biologically distinct diseases rather than a single molecular entity. The marked histology-specific differences in genomic alterations, immune microenvironment, and clinical outcomes support broader use of molecular characterization in these tumors and provide a rationale for histology- and biomarker-directed therapeutic development. Future studies integrating genomic profiling with treatment response will be critical to determine whether these biologic distinctions can be translated into more effective precision treatment strategies for patients with rare sinonasal malignancies.

Declarations

Conflict of interest disclosure:

Dr. Nabil Saba reports funding through federal grants UG1 CA233247, U54 CA274513, and grants from Exelixis and BMS, and having compensated or non-compensated advisory role with: Astra Zeneca, Eisai Medical, Exelixis, Merck, Merck EMD Serono, Pfizer, Kura, Vaccinex, CUE, BionTech, GSK, TOSK, Seagen, Flamingo, Infinity, Inovio, Aveo, Medscape, Onclive, Uptodate, BMS, J&J, Surface Oncology, Urogen, Summit,

Guidepoints, Astex, Imugene, Faron Pharmaceutical, Coherus, Adagene, Fulgent, Reddy Laboratories, Merus, Springer, Nanobiotix, Taiho. Dr. Nikki Schmitt reports research funding from Taiho Oncology, and consulting funding for Johnson & Johnson, GeoVax, Aspargo Labs. Drs. Adeyelu, Elliott, and Abdulla report employment and stocks with Caris Life Sciences.

Data sharing

The datasets generated and analyzed during this study are not publicly available as they contain proprietary molecular profiling data but are available from the corresponding authors or Caris Life Sciences subject to applicable institutional policies.

Declarations

Competing Interests

Dr. Nabil Saba reports funding through federal grants UG1 CA233247, U54 CA274513, and grants from Exelixis and BMS, and having compensated or non-compensated advisory role with: Astra Zeneca, Eisai Medical, Exelixis, Merck, Merck EMD Serono, Pfizer, Kura, Vaccinex, CUE, BionTech, GSK, TOSK, Seagen, Flamingo, Infinity, Inovio, Aveo, Medscape, Onclive, Uptodate, BMS, J&J, Surface Oncology, Urogen, Summit, Guidepoints, Astex, Imugene, Faron Pharmaceutical, Coherus, Adagene, Fulgent, Reddy Laboratories, Merus, Springer, Nanobiotix, Taiho. Dr. Nikki Schmitt reports research funding from Taiho Oncology, and consulting funding for Johnson & Johnson, GeoVax, Aspargo Labs. Drs. Adeyelu, Elliott, and Abdulla report employment and stocks with Caris Life Sciences.

Author Contribution

Concept and design: CES, NFS

Development and methodology: CES, BW, TA, AE, NFS

Acquisition of Data: TA, AE, FA, DL

Analysis and Data Interpretation: CES, BW, TA, AE, FA, NFS

Writing and Review of Manuscript: CES, BW, TA, EB, ALH, NCS, HMB, CAS, DMS, YT, JJ, CSF, DL, and NFS

Acknowledgments

The authors acknowledge the scientific, bioinformatics, pathology, and data analytics teams at Caris Life Sciences for generating and curating the comprehensive molecular profiling data used in this study.

References

1. Ferrari, M., et al., *Sinonasal Squamous Cell Carcinoma, a Narrative Reappraisal of the Current Evidence*. Cancers (Basel), 2021. 13(11).
2. Nightingale, J., et al., *Adenoid cystic carcinoma: a review of clinical features, treatment targets and advances in improving the immune response to monoclonal antibody therapy*. Biochim Biophys Acta Rev Cancer, 2021. 1875(2): p. 188523.
3. Persson, M., et al., *Rearrangements, Expression, and Clinical Significance of MYB and MYBL1 in Adenoid Cystic Carcinoma: A Multi-Institutional Study*. Cancers (Basel), 2022. 14(15).
4. Fujii, K., et al., *MYB, MYBL1, MYBL2 and NFIB gene alterations and MYC overexpression in salivary gland adenoid cystic carcinoma*. Histopathology, 2017. 71(5): p. 823–834.
5. Ho, A.S., et al., *The mutational landscape of adenoid cystic carcinoma*. Nat Genet, 2013. 45(7): p. 791–8.
6. Ho, A.S., et al., *Genetic hallmarks of recurrent/metastatic adenoid cystic carcinoma*. J Clin Invest, 2019. 129(10): p. 4276–4289.
7. Matsuki, T., et al., *PD-L1 expression as a predictive biomarker in patients with recurrent or metastatic salivary gland carcinoma treated with pembrolizumab*. Sci Rep, 2024. 14(1): p. 19794.
8. Resteghini, C., et al., *The SINTART 1 study. A phase II non-randomised controlled trial of induction chemotherapy, surgery, photon-, proton- and carbon ion-based radiotherapy integration in patients with locally advanced resectable sinonasal tumours*. Eur J Cancer, 2023. 187: p. 185–194.
9. Gray, S.T., et al., *Treatment outcomes and prognostic factors, including human papillomavirus, for sinonasal undifferentiated carcinoma: a retrospective review*. Head Neck, 2015. 37(3): p. 366–74.
10. Agaimy, A., et al., *SMARCB1 (INI-1)-deficient Sinonasal Carcinoma: A Series of 39 Cases Expanding the Morphologic and Clinicopathologic Spectrum of a Recently Described Entity*. Am J Surg Pathol, 2017. 41(4): p. 458–471.
11. Dogan, S., et al., *Frequent IDH2 R172 mutations in undifferentiated and poorly-differentiated sinonasal carcinomas*. J Pathol, 2017. 242(4): p. 400–408.
12. Ryu, H.J., C. Lee, and S.O. Yoon, *Epigenetic and Immune Profile Characteristics in Sinonasal Undifferentiated Carcinoma*. Cancer Med, 2024. 13(22): p. e70413.
13. Camisaschi, C., et al., *LAG-3 expression defines a subset of CD4(+)CD25(high)Foxp3(+) regulatory T cells that are expanded at tumor sites*. J Immunol, 2010. 184(11): p. 6545–51.
14. Xue, E., et al., *Genomic and Immune Correlates of EZH2 Expression and Activity in Olfactory Neuroblastoma*. Head Neck, 2026. 48(4): p. 932–940.
15. Wu, L., J. An, and H. Liu, *Clinicopathologic Features and Prognosis of Olfactory Neuroblastoma with Isocitrate Dehydrogenase 2 Mutations*. World Neurosurg, 2022. 159: p. e23-e31.
16. Classe, M., et al., *Integrated Multi-omic Analysis of Esthesioneuroblastomas Identifies Two Subgroups Linked to Cell Ontogeny*. Cell Rep, 2018. 25(3): p. 811–821 e5.
17. Gay, L.M., et al., *Comprehensive Genomic Profiling of Esthesioneuroblastoma Reveals Additional Treatment Options*. Oncologist, 2017. 22(7): p. 834–842.

18. Batchu, S., A.S. Gill, and M. Karsy, *Characterizing Immune Infiltration in Esthesioneuroblastoma Subtypes Through Gene Expression Deconvolution*. World Neurosurg, 2024. 183: p. e928-e935.
19. Saba, N.F., et al., *Neoadjuvant Chemotherapy and Surgery versus Surgery for Organ Preservation of T3 and T4a Nasal and Paranasal Sinus Squamous Cell Carcinoma: ECOG-ACRIN EA3163*. Clin Cancer Res, 2025. 31(12): p. 2339–2346.
20. Turner, J.H. and D.D. Reh, *Incidence and survival in patients with sinonasal cancer: a historical analysis of population-based data*. Head Neck, 2012. 34(6): p. 877–85.
21. Finotello, F., et al., *Molecular and pharmacological modulators of the tumor immune contexture revealed by deconvolution of RNA-seq data*. Genome Med, 2019. 11(1): p. 34.
22. Ayers, M., et al., *IFN-gamma-related mRNA profile predicts clinical response to PD-1 blockade*. J Clin Invest, 2017. 127(8): p. 2930–2940.
23. Ferrarotto, R., et al., *Clinical activity of REM-422, a MYB mRNA degrader, in recurrent/metastatic adenoid cystic carcinoma: Final results from the phase 1/2 dose-escalation cohort*. Journal of Clinical Oncology, 2026. 44.
24. Yang, Y., et al., *Genomic profiling and immune landscape of olfactory neuroblastoma in China*. Front Oncol, 2023. 13: p. 1226494.
25. Tandon, A. and A. Kakkar, *Sinonasal Undifferentiated and Poorly Differentiated Carcinomas: An Update*. Surg Pathol Clin, 2024. 17(4): p. 615–635.

Figures

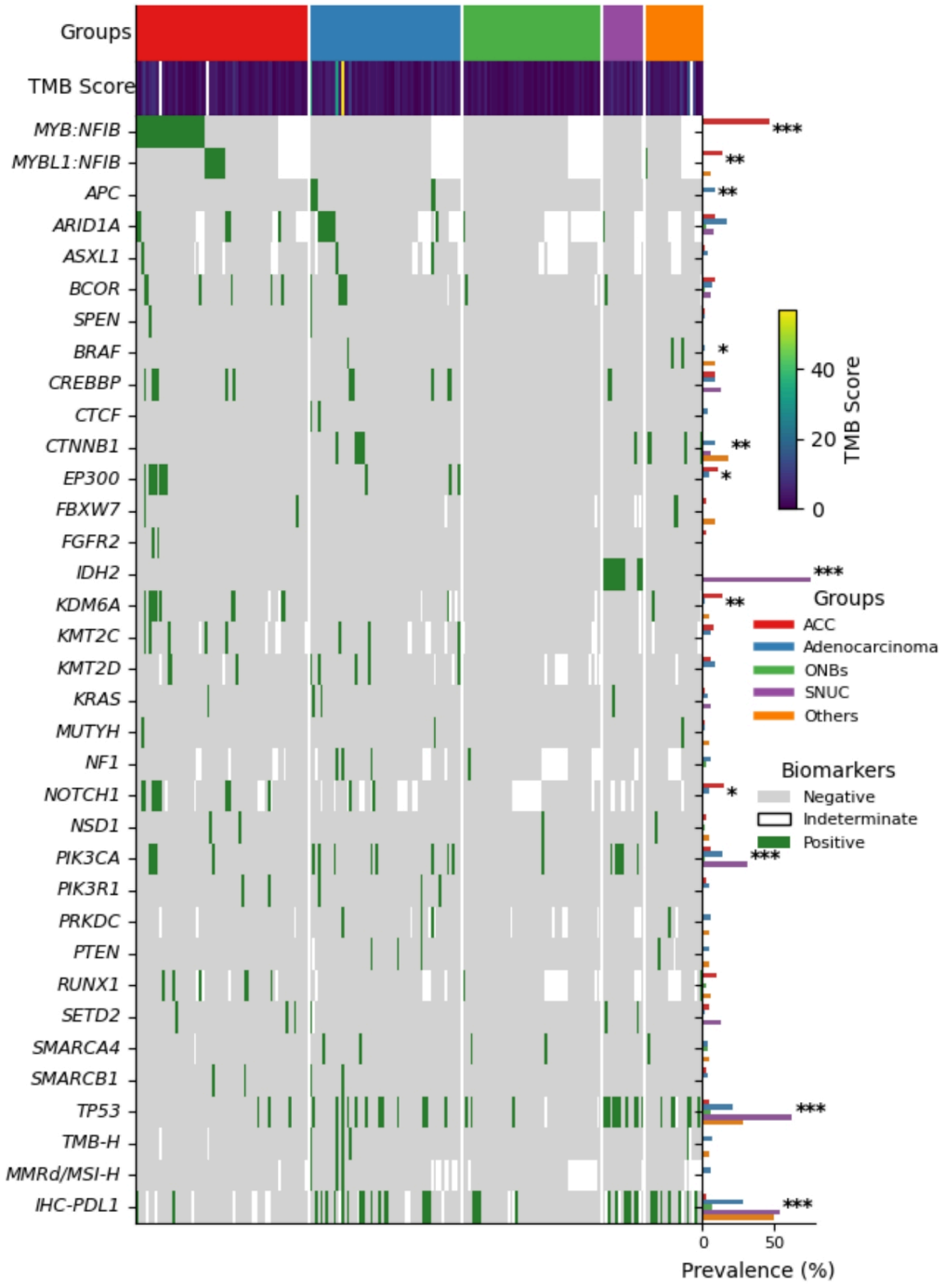


Figure 1

Genomic landscape across rare non-squamous sinonasal malignancies.
Comprehensive genomic profiling demonstrating recurrent genomic alterations across adenoid cystic carcinoma [8], adenocarcinoma, olfactory neuroblastoma (ONB), sinonasal undifferentiated carcinoma (SNUC), and other rare sinonasal histologies. The oncoprint displays the distribution and frequency of recurrent genomic alterations across individual tumors. *p<0.05, **p<0 .01, ***p<0.001, ****p<0.0001.

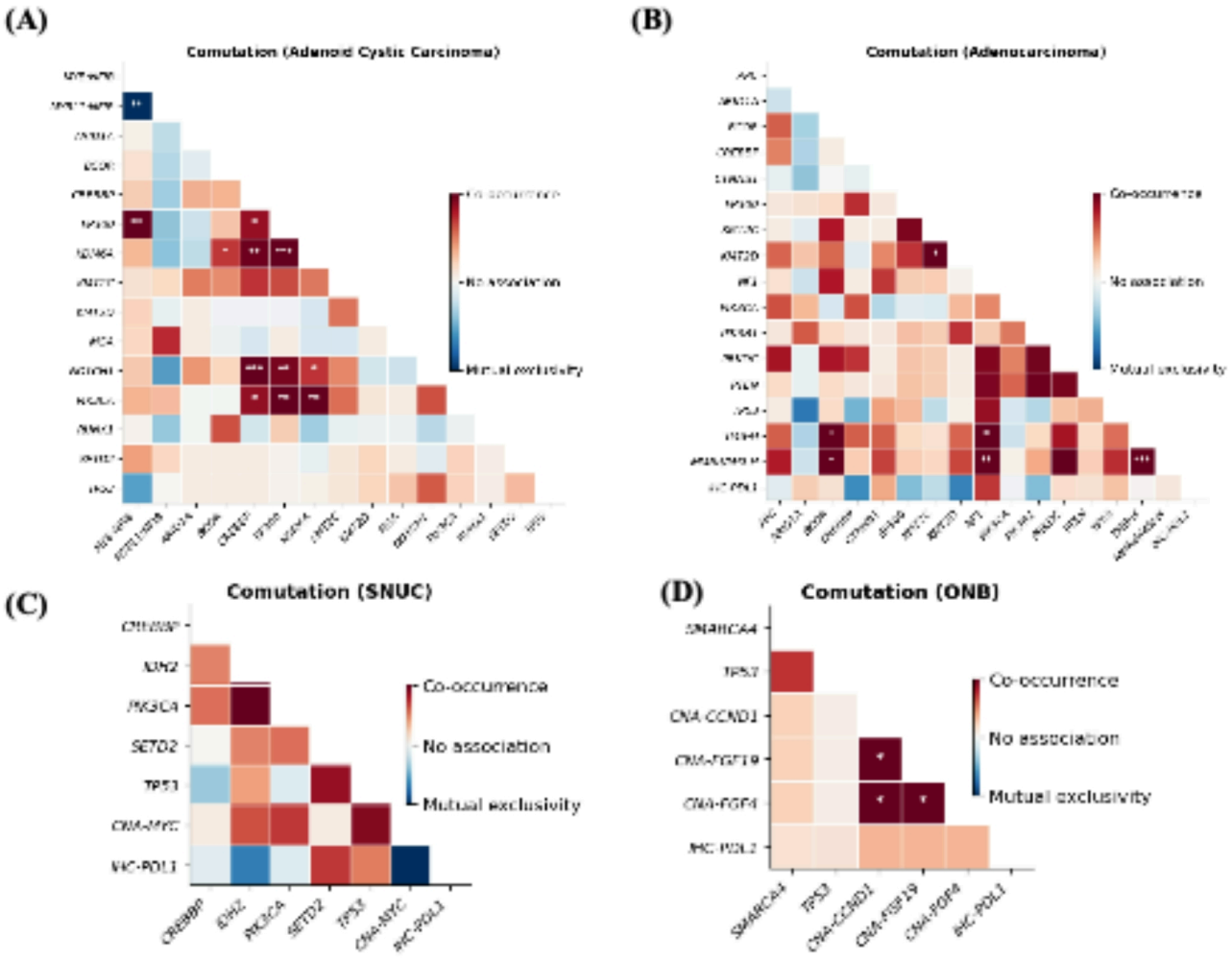


Figure 2

Co-mutation and mutual exclusivity analysis across sinonasal tumor subtypes.
Heatmaps demonstrating patterns of co-occurring and mutually exclusive genomic alterations within ACC (A), adenocarcinoma (B), SNUC (C), and ONB (D) cohorts. Red shading indicates increased co-occurrence between gene alterations, while blue shading indicates mutual exclusivity. Values represent log odds ratios derived from pairwise association analyses. Selected recurrent co-mutation relationships involving MYB/MYBL1-associated alterations, chromatin remodeling genes, TP53, APC, KRAS, and CDKN2A are highlighted across histologic subtypes.

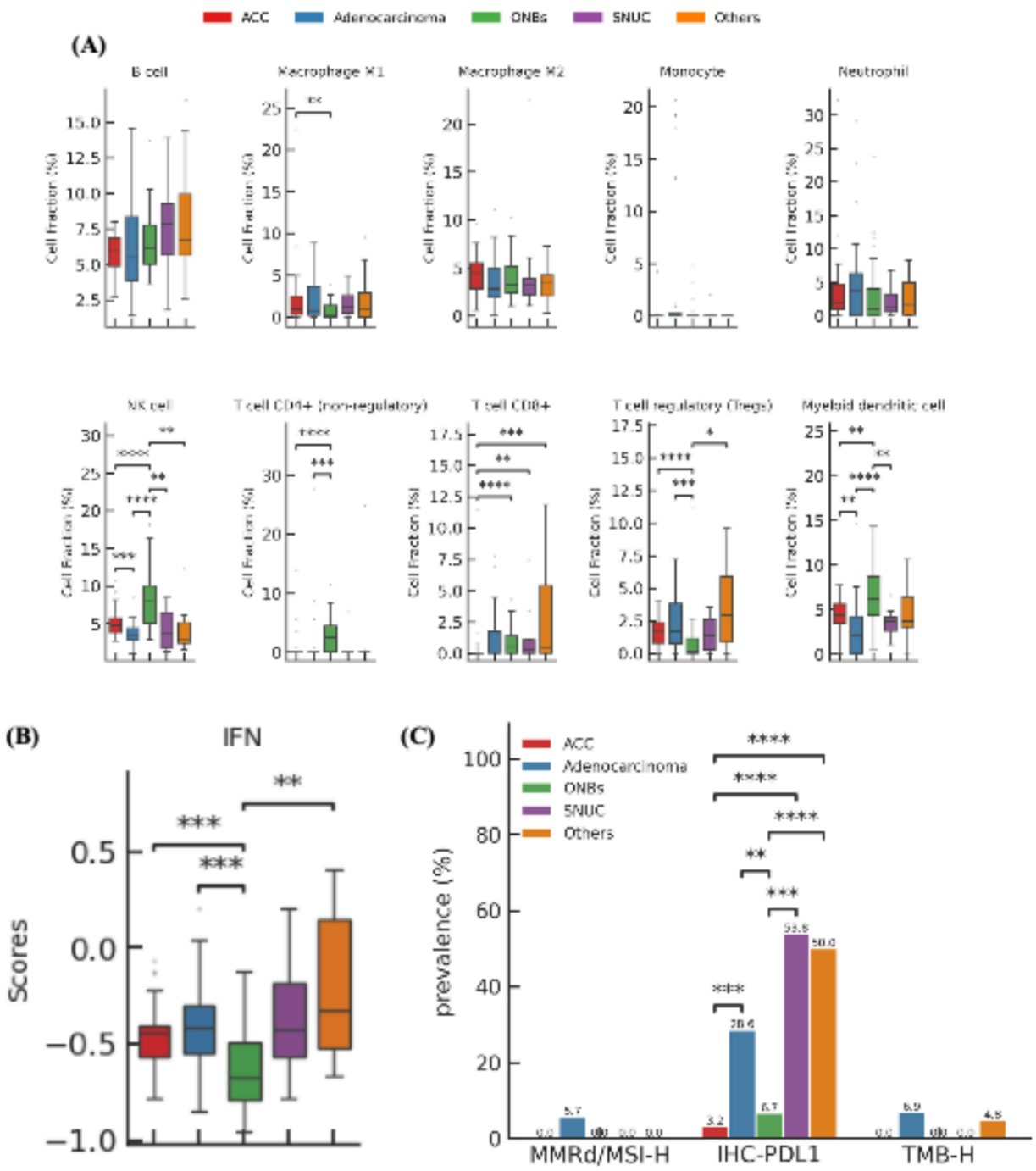


Figure 3

Tumor microenvironment profiling across rare non-squamous sinonasal malignancies. (A) Cell fractions were estimated using transcriptomic immune deconvolution analysis. (B) Interferon (IFN) signaling scores compared between different histologies. (C) Predictive biomarkers for immunotherapy response (TMB, PD-L1 and MMRd). *p<0.05, **p<0.01, ***p<0.001, ****p<0.0001.

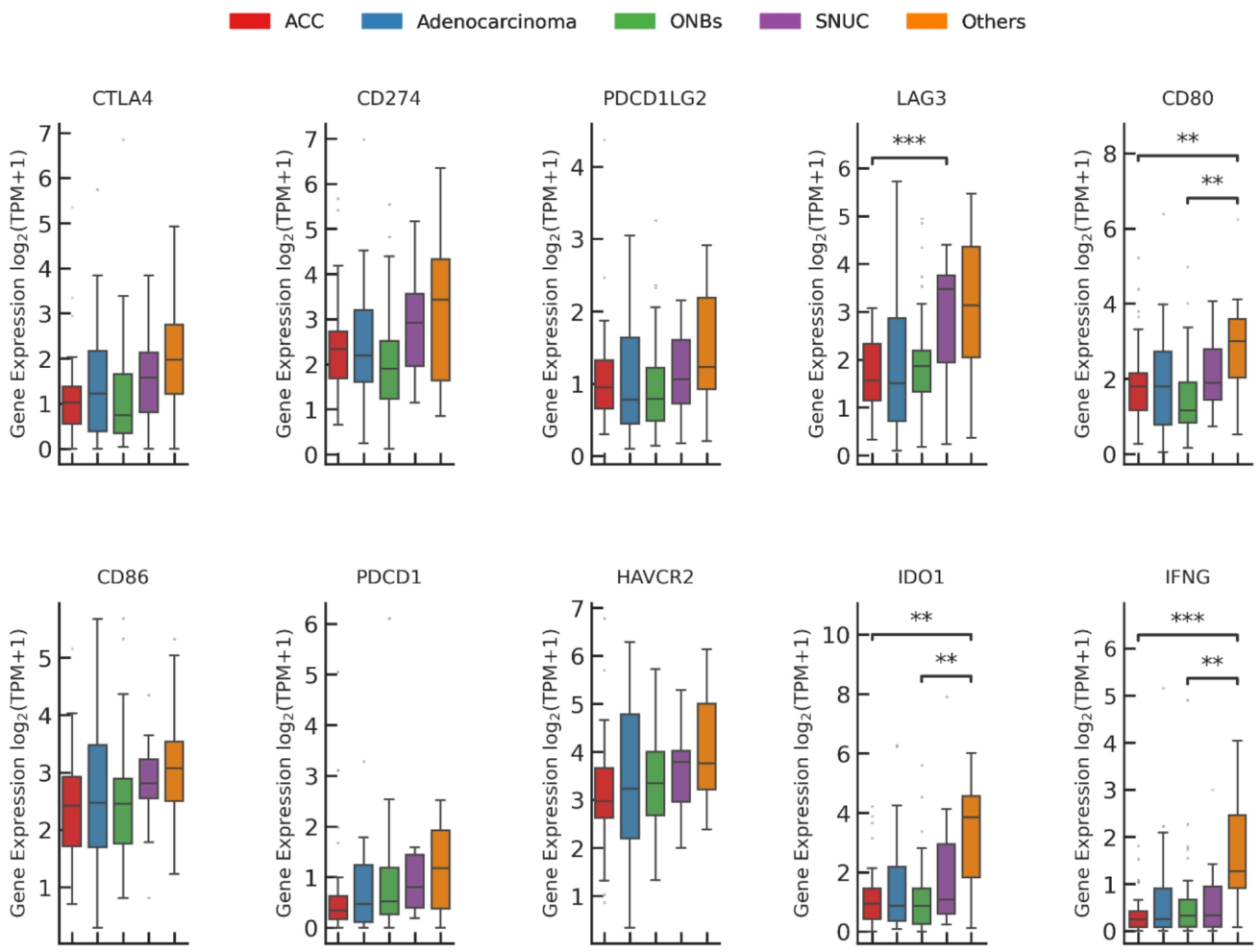
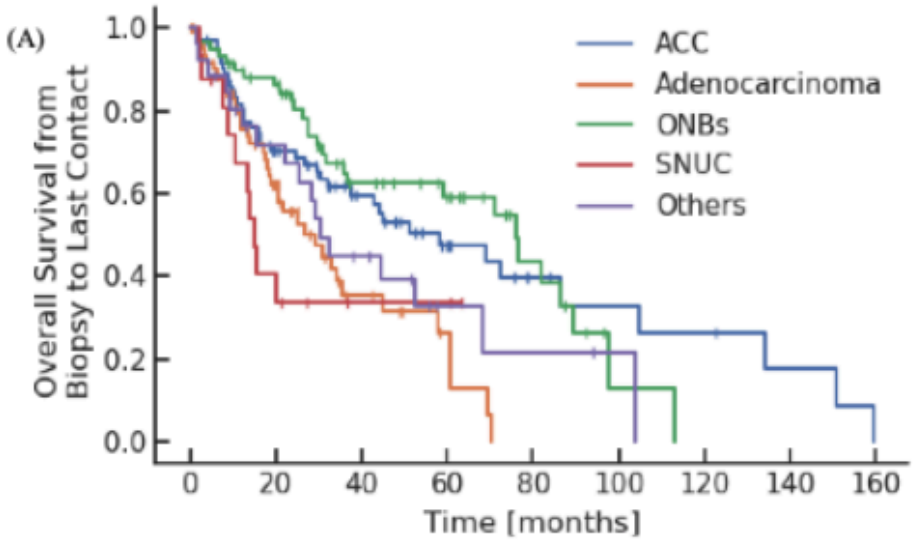
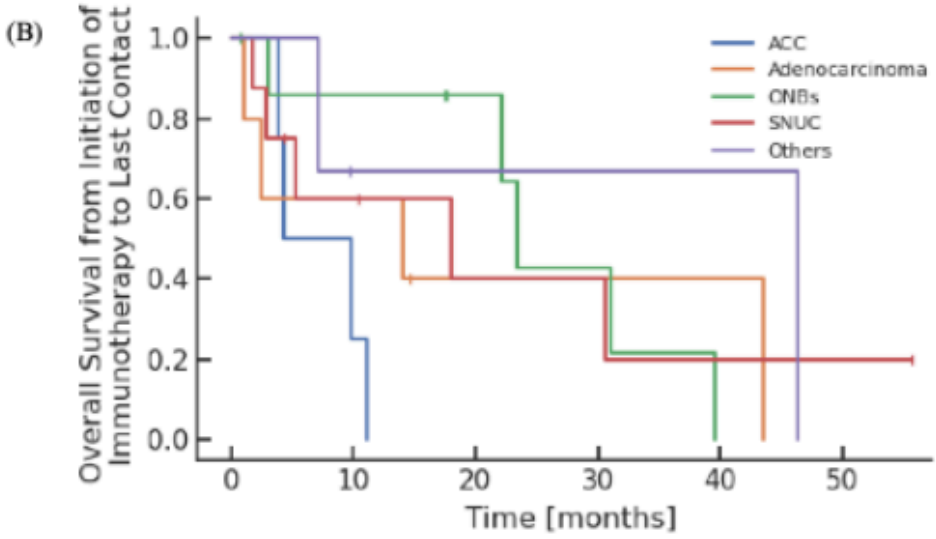


Figure 4

Immune checkpoint and immune regulatory gene expression across sinonasal tumor subtypes.
Differential expression of immune checkpoint and immune regulatory genes across ACC, adenocarcinoma, ONB, SNUC, and other sinonasal histologies. Boxplots depict normalized transcript expression levels for *CTLA4, CD274 (PD-L1), PDCD1LG2 (PD-L2), LAG3, CD80, CD86, PDCD1 (PD-1), HAVCR2 (TIM3), IDO1,* and*IFNG*. *p<0.05, **p<0.01, ***p<0.001, ****p<0.0001.



ACC (N = 72, mOS = 58.2mo); **Adenocarcinoma** (N = 62, mOS = 29.3mo); **ONB** (N = 62, mOS = 76.0mo); **SNUC** (N = 16, mOS = 14.9mo); **Others** (N = 26, mOS = 30.5mo). P<0.0001



ACC (N = 4, mOS = 4.2mo); **Adenocarcinoma** (N = 5, mOS = 14.1mo); **ONB** (N = 8, mOS = 23.4mo); **SNUC** (N = 8, mOS = 18.1mo); **Others** (N = 3, mOS = 46.4mo). P = 0.260

Figure 5

Overall survival analysis across rare non-squamous sinonasal malignancies.
Kaplan-Meier curves demonstrating overall survival across histologic subtypes using real-world insurance claims data. (A) Overall survival across the entire cohort. (B) Overall survival following initiation of immunotherapy. Number of patients and median overall survival are displayed for each histologic subtype. Statistical comparisons between groups were performed using the log-rank test. Abbreviations: ACC, adenoid cystic carcinoma; ONB, olfactory neuroblastoma; SNUC, sinonasal undifferentiated carcinoma; NR, not reached.

Supplementary Files

This is a list of supplementary files associated with this preprint. Click to download.

- SupplementaryData.docx